Journal of Sustainable Metallurgy
https://doi.org/10.1007/s40831-018-0164-6

SHORT COMMUNICATION

Sequential Extraction of Valuable Trace Elements from Bayer Process-Derived Waste Red Mud Samples

Hannian Gu[1] · Ning Wang[1] · Justin S. J. Hargreaves[2]

Abstract
Bayer Process-derived red mud produced in China can be classified into three types according to chemical composition: high-iron diaspore red mud, low-iron diaspore red mud, and gibbsite red mud. The specific chemical and mineral compositions of three such typical Bayer-derived red mud samples have been characterized by XRF, ICP-MS, XRD, and SEM. These results, for example, indicate that GX (a high-iron diaspore red mud) contains more than 1015 μg/g lanthanides, 313 μg/g yttrium, 115 μg/g scandium, and 252 μg/g niobium and that HN (a low-iron diaspore red mud) has a high content of lithium (224 μg/g), whereas SD (a gibbsite red mud) possesses a very low valuable trace element content, except for gallium (59.4 μg/g). A sequential extraction procedure was carried out to assess the leachability of valuable trace elements in these three red mud samples. Applying the extraction procedure, 60% of the yttrium in GX and 65% of the lithium in HN could be extracted which would be of interest for trace metal recovery.

Keywords Red mud · Leachability · Sequential extraction · Rare earth elements · Lithium

Introduction

Red mud is an aluminum industry-generated large-scale waste, which is primarily generated on a global scale by the Bayer process. However, large quantities of red mud are never used because of high costs and transportation difficulties [1–3]. In general, red mud comprises 6–8 main components and more than 50 trace elements. The contents of main components within different red mud samples vary in extremely broad ranges: for example, Al_2O_3 content ranges from 2.12–33.1 wt%, Fe_2O_3 from 6.8–71.9 wt%, and CaO in red mud can span in the range of 0.6–47.2 wt% [4]. Analogously, the concentration of trace elements (usually comprising less than 0.1–1.0 wt%) also has a wide range [2, 5], with examples of such trace elements being arsenic, beryllium, cadmium, chromium, copper, gallium, lead, lithium, manganese, mercury, nickel, potassium, scandium, thorium, uranium, vanadium, zinc, and zirconium as well as lanthanides. Both the main components and the trace elements in red mud can be extracted as resources. Hence, red mud can be regarded as a 'polymetallic raw material' or an 'artificial ore' source containing high amounts of valuable metals [6, 7]. Recovering the valuable metals from red mud is a potential choice to deal with the dilemma of natural ore shortages.

Conventional methods for leaching of elements from red mud have usually employed acid, alkali, or calcination processes to obtain the target products, aiming to investigate optimal leaching conditions. Previous literature relating to the use of Tessier's sequential extraction procedure [8–10] focused on the environmental impact on toxic elements (like Al, Cr, Ni, Zn, and Mn). It is necessary to know the speciation of valuable trace elements for recovery through leaching or extraction from red mud, since red mud can be classified into different types by chemical composition [11]. The present study reports the speciation

The contributing editor for this article was Brajendra Mishra.

Electronic supplementary material The online version of this article (https://doi.org/10.1007/s40831-018-0164-6) contains supplementary material, which is available to authorized users.

✉ Hannian Gu
guhannian@vip.gyig.ac.cn

[1] Key Laboratory of High-temperature and High-pressure Study of the Earth's Interior, Institute of Geochemistry, Chinese Academy of Sciences, Guiyang 550081, People's Republic of China

[2] West CHEM, School of Chemistry, Joseph Black Building, University of Glasgow, Glasgow G12 8QQ, UK

Published online: 12 February 2018

of valuable trace elements in red mud as well as the variations of different red mud types as a function of sequential extraction stage. The aim of the present study was to assess the leachability of valuable trace elements in red mud, and to compare the fractionation and speciation of valuable trace elements in red mud from different origins in China. For this purpose, a modification of Tessier's sequential extraction procedure [12] was applied to estimate the leachability of valuable trace elements.

Materials and Methods

Samples and Characterization Methods

The Bayer process-derived red mud obtained in China can be classified into three types by chemical composition: high-iron diaspore red mud, low-iron diaspore red mud, and red mud generated from imported gibbsite [11]. Three such red mud samples drawn from three locations were used in this study: GX (from Guangxi, China, a high-iron diaspore red mud), HN (from Henan, China, a low-iron diaspore red mud), and SD (from Shandong, China, a red mud generated from imported gibbsite). For the purposes of comparison, the elemental compositions determined for a range of different red mud samples are presented in Table S1 (Supplementary Material).

The main chemical compositions of the three samples were determined using X-Ray Fluorescence Spectroscopy (XRF, Philips PW2404); inductively coupled plasma-atomic emission spectrometry (ICP-AES, Agilent VISTA) or inductively coupled plasma-mass spectrometry (ICP-MS, Perkin Elmer Elan 9000) were used to analyze trace chemical compositions of the various samples. Prepared samples were fused with a lithium metaborate–lithium tetraborate flux which also included an oxidizing agent (lithium nitrate), and were then poured into a platinum mold. The resultant disk was in turn analyzed by XRF spectrometry. The XRF analysis was determined in conjunction with a loss-on-ignition at 1000 °C. The lithium and scandium concentrations in the solid red mud and final residue samples were obtained by ICP-AES. Specifically, a prepared sample was digested with perchloric, nitric, and hydrofluoric acids. The residue was then leached with dilute hydrochloric acid and diluted to produce a known volume which was then analyzed by ICP-AES. Results were corrected for complications arising from spectral inter-element interference. Trace elements, with the exceptions of lithium and scandium, in the solid red mud and final residue samples were determined as follows: each sample was added to a lithium metaborate/lithium tetraborate flux, mixed well, and fused in a furnace at 1025 °C. The resulting melt was then cooled and dissolved in an acid mixture containing nitric, hydrochloric, and hydrofluoric acids. Finally, the solution was analyzed by ICP-MS.

All three red mud samples were characterized by powder X-ray diffraction (XRD) with measurements being performed using a Siemens D5000 diffractometer with Cu Kα radiation. A 2θ range between 5° and 85° was scanned using a counting rate of 1 s per step with a step size of 0.02°. Samples were prepared by compaction into a silicon sample holder. For SEM observation, samples were imaged in an FEI Scios scanning electron microscope.

Sequential Extraction Procedure

Leachability amounts of valuable trace elements in all the three red mud samples were evaluated by a modified sequential extraction procedure. To Tessier's original partitioning scheme, extraction with water was added as an initial step. After mechanical shaking, centrifugation, and filtration, the concentrations of elements in each particular fraction were determined by ICP-MS. The solid residues remaining after each extraction step were washed with 15 mL of water, shaken for 15 min, centrifuged at 3500 rpm for 3 min, decanted, and the washing solution discarded prior to the addition of the next extractant (Fig. 1). After each extraction step, the leachate was separated from the residue by filtering through a 0.45-μm Millipore filter paper using a glass Millipore vacuum filter assembly. The leachate was stored for trace element analysis (ICP-MS and ICP-AES), and the residue on the filter paper was carried over to the next step of sequential extraction. Each analysis performed in this study was conducted once.

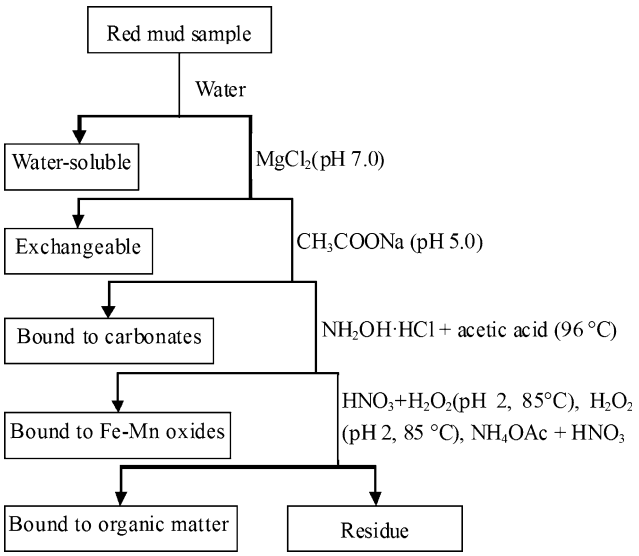

Fig. 1 Flow sheet of the sequential extraction procedure for the red mud samples

Water-Soluble Fraction

In this section, 3.00 g of each red mud sample was transferred into a 50-mL polypropylene centrifuge tube, and the sample was shaken for 24 h with 30 mL of water, centrifuged, decanted, and filtered.

Exchangeable Fraction

The extraction solution applied was 30 mL of 1 M magnesium chloride ($MgCl_2$) at pH 7.0, with the residue being shaken for 24 h at room temperature, centrifuged, decanted and filtered.

Fraction Bound to Carbonates

The extraction solution applied was 30 mL of 1 M sodium acetate (CH_3COONa) adjusted to pH 5.0 with acetic acid, and the residue was shaken for 24 h at room temperature, centrifuged, decanted, and filtered.

Fraction Bound to Fe–Mn Oxides

The extraction solution applied was 30 mL of 0.03 M hydroxylamine hydrochloride ($NH_2OH{\cdot}HCl$) in 25% (v/v) acetic acid. Extraction was carried out at 96 ± 1 °C for 6 h with occasional agitation on a magnetic stirrer provided with a heater. After cooling to room temperature, the sample was centrifuged, decanted, and filtered.

Fraction Bound to Organic Matter

To the residue from the previous step was added 9 mL of 0.02 M HNO_3 and 15 mL of 30% H_2O_2 adjusted to pH 2 with HNO_3, and the mixture was heated to 85 ± 1 °C for 2 h with occasional agitation. A second 9 mL aliquot of 30% H_2O_2 (adjusted to pH 2 with HNO_3) was then added, and the sample was heated again to 85 ± 1 °C for 3 h with intermittent agitation. After cooling, 15 mL of 3.2 M NH_4OAc in 20% (v/v) HNO_3 was added, and the sample was diluted to 60 mL and agitated continuously for 30 min. Then, the sample was centrifuged, decanted, and filtered.

Residue

After drying the residue from prior step, the solid material obtained was determined by ICP-AES or ICP-MS.

Results and Discussion

Main Chemical Composition

The main chemical compositions of the three typical Bayer red mud samples used in this study are shown in Table 1. It can be seen that GX (the high-iron diaspore red mud) and SD (the red mud generated from gibbsite) possess higher iron contents than HN (the low-iron diaspore red mud) does. High iron content red muds, like GX and SD, can be considered an iron resource in situations where the recovery process is both economically and environmentally acceptable [13, 14]. HN and most red muds generated in China, similar to Guizhou red mud [15], have low iron contents. Hence, in general, in the context within China, iron recovery is not an economic choice for complete utilization. Another difference in the content of the samples examined within the present study relates to CaO. In the table, it can be seen that the CaO content of SD is 1.5 wt%, which is far lower than those for GX and HN. Calcium (lime) is commonly added during the Bayer Process so as to aid in processing [16]. Lower amounts of calcium added in the Bayer process may have the result that less sodium could be recycled resulting in a higher sodium content in red mud, e.g., in SD.

Trace Chemical Composition

Red mud contains many metals in trace amounts, and these can be classified into three types: (i) valuable trace metals, such as rare earth elements and gallium; (ii) toxic or radioactive trace metals, such as chromium, uranium and thorium; and (iii) other trace metals, such as strontium and barium. However, of course, toxic or radioactive trace metals can also be valuable if their concentration is high enough for recovery, as would be the case, for instance, for

Table 1 The main chemical compositions of three typical Bayer-derived red mud samples sourced from China (wt%)

	Al_2O_3	SiO_2	Fe_2O_3	CaO	TiO_2	Na_2O	K_2O	MgO	BaO	Cr_2O_3	MnO	P_2O_5	SO_3	SrO	LOI
GX	17.57	12.77	29.76	14.30	6.08	5.07	0.22	0.66	0.01	0.25	0.14	0.14	0.59	0.02	11.58
HN	22.54	19.70	9.69	17.65	4.12	6.82	2.10	1.44	0.01	0.06	0.03	0.20	1.30	0.08	13.31
SD	21.98	17.16	33.25	1.50	4.76	9.33	0.17	0.12	< 0.01	0.05	0.06	0.13	0.30	< 0.01	10.39

Table 2 Concentrations of lanthanides and other trace elements in the three red mud samples (μg/g)

Element Accuracy	La 0.5	Ce 0.5	Pr 0.03	Nd 0.1	Sm 0.03	Eu 0.03	Gd 0.05	Tb 0.01	Dy 0.05	Ho 0.01	Er 0.03	Tm 0.01	Yb 0.03	Lu 0.01	La–Lu
GX	214	483	31.4	99.5	21.6	4.87	26.1	6.05	44.2	10.10	30.5	5.02	33.7	5.16	1015.20
HN	165.5	356	35.3	114.5	19.10	3.86	15.30	2.59	15.70	3.27	9.42	1.49	10.05	1.56	753.64
SD	31.6	127.0	7.79	27.5	6.07	1.65	6.88	1.46	10.05	2.34	7.12	1.19	7.97	1.30	239.92
Element Accuracy	Cr 10	Cs 0.01	Ga 0.1	Hf 0.2	Nb 0.2	Rb 0.2	Sn 1	Ta 0.1	Th 0.05	U 0.05	V 5	Y 0.5	Zr 2	Li 0.2	Sc 0.1
GX	1920	3.22	49.9	77.1	313	17.8	35	23.1	117.5	34.4	491	252	2720	50.0	115.5
HN	510	1.86	47.8	32.3	108.0	55.9	20	8.5	111.0	33.3	394	83.9	1090	224	66.2
SD	430	1.01	59.4	35.6	56.4	10.0	23	4.5	56.9	9.11	602	64.1	1280	6.0	54.4

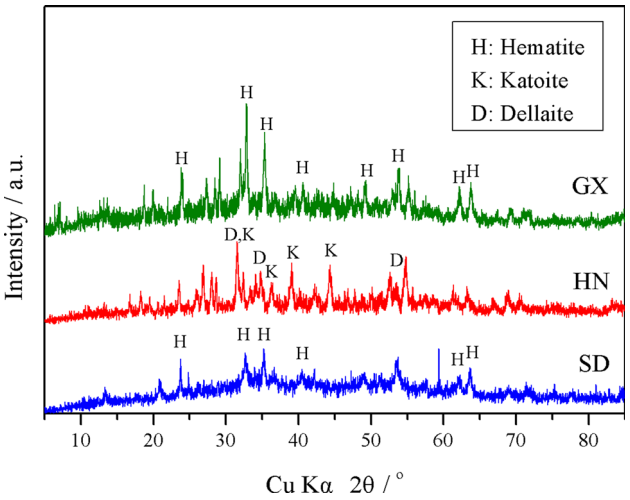

Fig. 2 Powder X-ray diffraction patterns of red mud samples

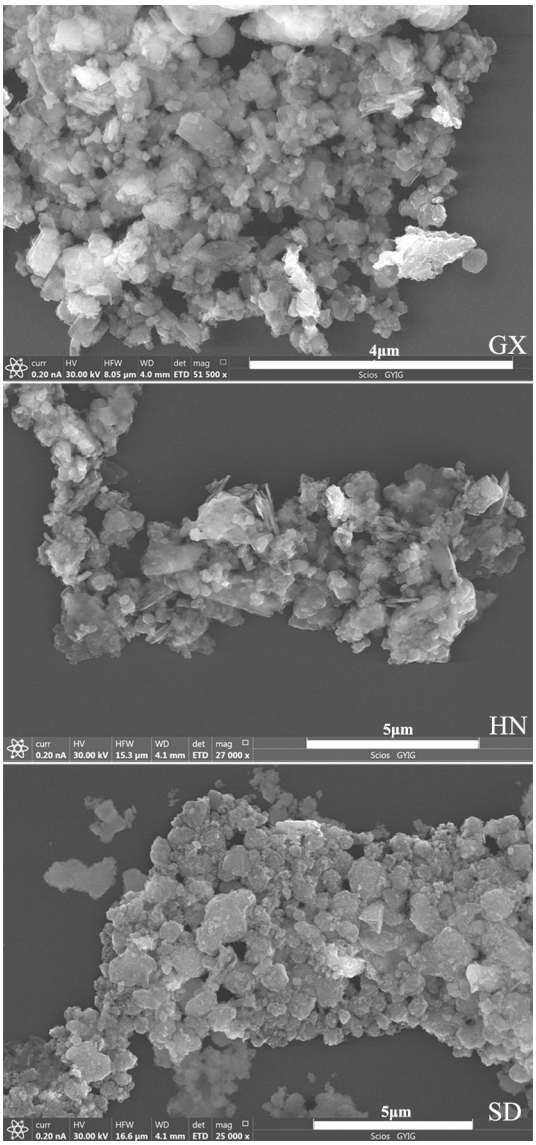

Fig. 3 SEM images of red mud samples

uranium and thorium. In the context of extraction of value from waste red mud, it is particularly notable that rare earth elements (REEs, including the lanthanides, scandium, and yttrium) are viewed as 'critical metals' due to the currently prevailing complex array of production and political issues in relation to them. Red mud has been considered to be a REE resource [17].

The trace chemical compositions of the red mud samples analyzed in this study are presented in Table 2. As seen in Table 2, GX contains 1015.2 μg/g lanthanides, 115.5 μg/g scandium, 252 μg/g yttrium, and 313 μg/g niobium. In general, high-iron diaspore red mud tends to comprise more rare earth metals, thorium, uranium, niobium, and tantalum. Notably, HN has an anomalous lithium content of 224 μg/g. Although lithium has seldom been reported as a potential resource in red mud, it can be present in bauxite [18]. Compared with GX and HN, the gibbsite red mud SD has very low contents of trace metals, their concentrations usually being lower than those in diaspore red mud with the exception of gallium and vanadium, among others.

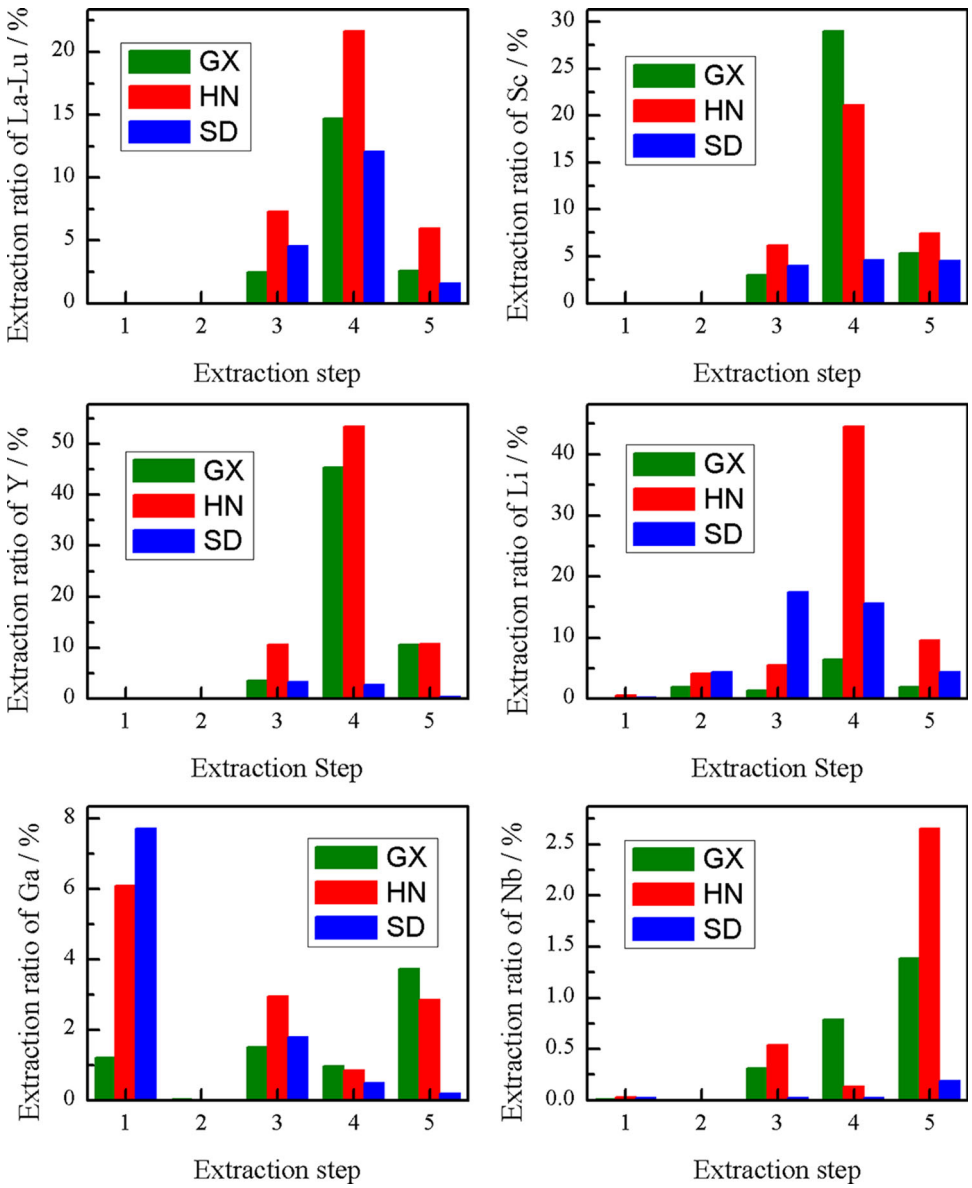

Fig. 4 Partitioning of valuable elements in GX, HN, and SD on applying the modified Tessier's extraction procedure. *1* water-soluble, *2* exchangeable, *3* bound to carbonates, *4* bound to Fe–Mn oxides, and *5* bound to organic matter fractions

Like most of the main chemical compositional elements, the trace elements are derived from bauxite ore, and their concentrations differ significantly depending on the parent ore source and hence on their composition. For extraction or recovery of valuable elements, it is crucial to have an awareness of the form in which they occur, the distribution of elements, and also the type of red mud.

Mineral Composition

Red mud samples were characterized by powder X-ray diffraction (shown in Fig. 2).The XRD patterns of GX and SD have been previously reported in the context of iron-containing phase identification [19]. The identity and quantity of mineralogical components in red mud are diverse and not easy to determine [4]. The main reflections in the patterns of GX and SD match well with hematite, while HN consists of compounds containing calcium, aluminum, and silicon, such as katoite ($Ca_3Al_2(OH)_{12}$, PDF: 24-0217) and dellaite ($Ca_6Si_2O_7SiO_4(OH)_2$, PDF: 74-1995). The mineral-phase composition of low iron content red mud is much more complex than that of high iron content red mud. The differences are reflected in the particles' morphologies of red mud samples (Fig. 3). Particles of GX are granular, well crystallized with different sizes, while minerals in SD do not have clear crystal edge with similar sizes. In addition, minerals in HN have shapes of large block, small granularity, and schistose structure.

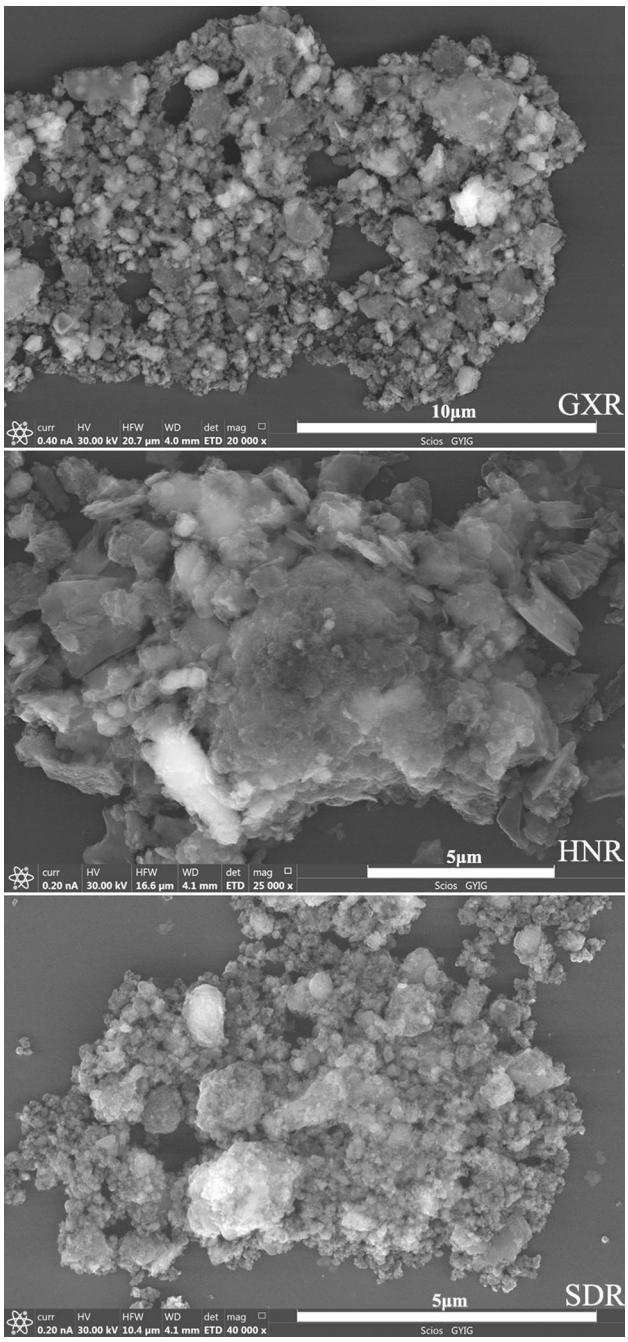

Fig. 5 SEM images of final residues after leaching. GXR, GX residue; HNR, HN residue; SDR, GX residue

Leachability of Valuable Elements

The leachability of the different valuable metals present in GX, HN, and SD was evaluated by the sequential extraction procedure detailed in the experimental section, and the leachability of the lanthanides, scandium, yttrium, lithium, gallium, and niobium from the three red mud samples is presented in Fig. 4.

The lanthanides (La-Lu, not including Pm) can be extracted in the final three steps of sequential extraction procedure, with the greatest amount being removed in the fourth step (i.e., that bound to Fe–Mn oxides). Although HN does not contain the highest lanthanide content of the three red mud samples, 35% of these metals could be leached, with 22% being in the fraction bound to Fe–Mn oxides. The general trend in extractions of scandium and yttrium from the different red mud samples is similar to that of the lanthanides. Conversely, the total proportion of scandium in GX extracted was 37%, exceeding only very slightly that for the HN sample (35%). It is noteworthy that the leachability values of yttrium in GX and HN are remarkably high, being 60 and 75%, respectively. As discussed above, the yttrium content in GX is as high as 252 μg/g. Hence, the recovery of valuable yttrium is significant in that 60% of yttrium can be recovered in total, with 45% being removed in the fraction bound to Fe–Mn oxides using hydroxylamine hydrochloride solution. The present study is focused on the speciation of valuable trace elements in red mud and their individual variations between different types of red mud. It demonstrates that the sequential extraction procedure undertaken might be an avenue worthy of further exploration. To develop viable extraction processes, further research is required, e.g., improvement of the leaching yields by changing the amounts of reagents, and separating from other elements present.

Lithium has been recognized as a potentially critical raw material because of its wide-ranging and growing uses, and the increasing demand for lithium may lead to a greater emphasis upon lithium recovery from smaller mineral deposits and also byproducts [20]. Lithium can be observed in solution from all of the five steps based on the sequential extraction procedure, and in general, predominant extraction is associated with the fourth step. The total amount of lithium removed from HN was as high as 65%, with 45% originating in the fourth step. Given that the lithium content in HN is 224 μg/g, the leachability of lithium observed

Table 3 Major chemical compositions of the final residues following the extraction procedure (wt%)

	Al_2O_3	Fe_2O_3	CaO	TiO_2	Na_2O	K_2O	MgO	P_2O_5	SO_3
GXR	9.10	34.00	2.24	7.78	0.38	0.1	0.37	0.337	0.05
HNR	17.8	10.74	1.61	5.30	0.35	1.9	1.17	0.417	0.08
SDR	14.5	36.86	0.07	5.08	0.12	0.2	0.10	0.302	0.05

Table 4 Trace element compositions of the final residues following the extraction procedure (μg/g)

Element	La	Ce	Pr	Nd	Sm	Eu	Gd	Tb	Dy	Ho	Er	Tm	Yb	Lu	La–Lu
Accuracy	0.5	0.5	0.03	0.1	0.03	0.05	0.01	0.05	0.01	0.03	0.01	0.03	0.01	0.5	
GXR	237	624	30.8	101.5	22.4	21.7	4.77	34.3	7.12	20.5	3.18	20.8	3.06	237	1131.1
HNR	147.5	399	29.2	91.8	14.90	8.78	1.56	9.46	1.86	4.93	0.75	4.79	0.70	147.5	715.23
SDR	26.4	135.5	5.78	20.7	5.22	6.90	1.53	11.91	2.78	8.55	1.45	9.65	1.51	26.4	237.88

Element	Cr	Cs	Ga	Hf	Nb	Rb	Sn	Ta	Th	U	V	Y	Zr	Li	Sc
Accuracy	10	0.01	0.1	0.2	0.2	0.2	1	0.1	0.05	0.05	5	0.5	2	0.2	0.1
GXR	1670	1.74	67.6	91.6	442	9.2	45	26.9	148.5	14.64	389	136	3780	47.5	81.1
HNR	410	1.52	61.2	38.4	137.5	51.1	24	10.0	136.0	9.57	277	34.4	1510	110	56.2
SDR	450	1.10	75.8	39.7	70.7	9.9	35	5.1	65.2	7.42	591	74.4	1640	4.3	70.8

is potentially attractive for lithium recovery. Gallium and niobium presented different leaching trends; for instance, 7.7% of gallium present in the SD sample was leached in the water-soluble step, and 2.65% of the niobium present in the HN sample was leached in the fifth step (i.e., the fraction bound to organic matter).

Final Residues

The morphologies of the final residues from the three samples were investigated, and the resultant SEM images are presented in Fig. 5. To more fully understand the extraction process, some major elements were determined using ICP-AES or ICP-MS, and Table 3 presents compositions expressed in the form of oxides. The contents of trace elements in the final residues were determined to confirm the changes occurring during the leaching process, and the results are shown in Table 4. In comparison to Table 2, it can be observed that some trace elements, such as gallium and niobium, were enriched in the final residue since only a minor fraction of them was extracted during the leaching process. Conversely, net depletion is observed in the case of other elements such as yttrium and lithium for which major fractions are leached. For the lanthanide content, there was little overall change in the final residues with respect to that in the red mud samples from which they were derived. In the case of some elements, the remaining amounts in the residues were dependent on the identity of the red mud parent samples. Such a situation arises in the case of scandium, for instance, where its concentration is decreased in the residues of GX and HN, but enhanced in the SD residue.

Conclusions

Red mud contains numerous valuable trace metals with high-iron diaspore red muds in particular possessing a higher concentration of valuable trace metals compared to other forms of red muds. The high-iron diaspore red mud GX in the present study comprises 1015.2 μg/g lanthanides, 115.5 μg/g scandium, 252 μg/g yttrium, and 313 μg/g niobium, while the low-iron diaspore red mud (HN) investigated has a high lithium content (224 μg/g). Hematite is the main mineral phase of the gibbsite red mud investigated (SD), and this kind of red mud possesses lower valuable trace element content for potential utilization. It has been demonstrated that 60% of the yttrium in GX and 65% of the lithium in HN can be recovered, and such an extent of recovery proves to be of potential interest.

Acknowledgements The authors would like to acknowledge the financial supports from the National Natural Science Foundation of China (Grant No. 41402039), and Guizhou Provincial Science and Technology Foundation (No. J [2016] 1155). The authors are grateful to Dr W. Liu who provided the red mud samples.

References

1. Wang S, Tadé A, Tadé MO (2008) Novel applications of red mud as coagulant, adsorbent and catalyst for environmentally benign processes. Chemosphere 72:1621–1635
2. Liu Y, Naidu R, Ming H (2011) Red mud as an amendment for pollutants in solid and liquid phases. Geoderma 1(63):1–12
3. Borra CR, Blanpain B, Pontikes Y, Binnemans K, Van Gerven T (2016) Recovery of rare earths and other valuable metals from bauxite residue (red mud): a review. J Sustain Metall 2:365–386
4. Gräfe M, Power G, Klauber C (2011) Bauxite residue issues: III. Alkalinity and associated chemistry. Hydrometallurgy 108:60–79
5. Evans K (2016) The history, challenges, and new developments in the management and use of bauxite residue. J Sustain Metall 2:316–331
6. Klauber C, Gräfe M, Power G (2011) Bauxite residue issues: II. options for residue utilization. Hydrometallurgy 108:11–32
7. Davris P, Balomenos E, Panias D, Paspaliaris I (2016) Selective leaching of rare earth elements from bauxite residue (red mud), using a functionalized hydrophobic ionic liquid. Hydrometallurgy 164:125–135
8. Ghosh I, Guha S, Balasubramaniam R, Kumar AVR (2011) Leaching of metals from fresh and sintered red mud. J Hazard Mater 185:662–668

9. Milačič R, Zuliani T, Ščančar J (2012) Environmental impact of toxic elements in red mud studied by fractionation and speciation procedures. Sci Total Environ 426:359–365
10. Gu H, Wang N (2013) Leaching of uranium and thorium from red mud using sequential extraction methods. Fresen Environ Bull 22(9a):2763–2769
11. Liu W, Chen X, Li W, Yu Y, Yan K (2014) Environmental assessment, management and utilization of red mud in China. J Clean Prod 84:606–610
12. Tessier A, Campbel PGC, Bisson M (1979) Sequential extraction procedure for the speciation of particulate trace metals. Anal Chem 51(7):844–851
13. Gu H, Hargreaves JSJ, JiangJ-Q Rico JL (2017) Potential routes to obtain value-added iron-containing compounds from red mud. J Sustain Metall 3(3):561–569
14. Samouhos M, Taxiarchou M, Pilatos G, Tsakiridis PE, Devlin E, Pissas M (2017) Controlled reduction of red mud by H_2 followed by magnetic separation. Miner Eng 105:36–43
15. Gu H, Wang N, Liu S (2012) Characterization of Bayer red mud from Guizhou, China. Miner Metall Proc 29(3):169–171
16. Smith P (2017) Reactions of lime under high temperature Bayer digestion conditions. Hydrometallurgy 170:16–23
17. Deady ÉA, Mouchos E, Goodenough K, Williamson BJ, Wall F (2016) A review of the potential for rare-earth element resources from European red muds: examples from Seydişehir, Turkey and Parnassus-Giona, Greece. Mineral Mag 80(1):43–61
18. Wang D, Li P, Qu W, Yin L, Zhao Z, Lei Z, Wen S (2013) Discovery and preliminary study of the high tungsten and lithium contents in the Dazhuyuan bauxite deposit, Guizhou, China. Sci China Earth Sci 56(1):145–152
19. Gu H, Hargreaves JSJ, McFarlane AR, MacKinnon G (2016) The carbon deposits formed by reaction of a series of red mud samples with methanol. RSC Adv 6(52):46421–46426
20. Reichel S, Aubel T, Patzig A, Janneck E, Martin M (2017) Lithium recovery from lithium-containing micas using sulfur oxidizing microorganisms. Miner Eng 106:18–21